Landscape and Urban Planning 240 (2023) 104880

Contents lists available at ScienceDirect

Landscape and Urban Planning

journal homepage: www.elsevier.com/locate/landurbplan

Visual Capital: Evaluating building-level visual landscape quality at scale

Adam R. Swietek [a,*], Marius Zumwald [b]

[a] Laboratory of Environmental and Urban Economcs, Institute of Architecture, School of Architecture, Civil and Environmental Engineering, EPFL (École Polytechnique Fédérale de Lausanne), Lausanne, Switzerland
[b] Wüest Partner, Zurich, Switzerland

HIGHLIGHTS

- 3D building view-metrics are computed using a large-scale digital model.
- Visual capital is measured by calibrating view-metrics with average net-income.
- Water and distant views strongly influence visual capital.
- Visual capital is context-dependent, relying on combinations of individual view elements.
- The urban and natural form influence the scarcity of a good view, i.e. view-inequality.

ARTICLE INFO

JEL classification:
C21
C55
Q56
Q57
R23
R30

Keywords:
3D spatial metrics
Preference
Natural capital
GeoAI
Spatial analysis
Urban economics

ABSTRACT

Evaluating visual landscape quality provides valuable information for urban development and spatial planning. In practice however, obtaining high resolution view-metrics and outcome data with sufficient geographic coverage has remained challenging. To overcome this limitation, we construct a scalable measure of visual landscape quality by first defining building-level view-metrics derived from a large-scale 3D representation of Switzerland's building stock. Leveraging the principle of income-sorting, we estimate visual preferences by calibrating the building level view-metrics with commune-level incomes (CLI). The learned model captures common intuition on visual preferences, i.e. attributing positive weight to lake-views, and identifies context-dependent relationships between view metrics. To contextualize the derived quantitative measure, we refer to the preference for a building's portfolio of viewpoints as a building's visual capital (VC). By assessing the supply of VC across Switzerland's entire building stock, we uncover an association between VC and the urban and natural form, where urban density and landscape topology explain the strength of view-driven-income sorting across agglomerations. We demonstrate that spatial clustering of VC varies across cities and frequently crosses administrative boundaries. Finally, we release a privacy protected version of VC at www.visualcapital.xyz, which we expect to promote future interdisciplinary studies focused on correlates of visual landscape quality (whether financial, social, environmental or physiological).

1. Introduction

To estimate the revealed preference for housing views and visual landscape, defined as the geographic areas visible as perceived by an observer from one or more viewpoints (Inglis, Vukomanovic, Costanza, & Singh, 2022), it is common to use the hedonic pricing model to calculate the marginal effect of a derived view indicator on real estate transaction prices (Baranzini & Schaerer, 2011; M. Chen, Liu, Arribas-Bel, & Singleton, 2022; Law, Paige, & Russell, 2019; Turan, Chegut, Fink, & Reinhart, 2021; Yamagata, Murakami, Yoshida, Seya, & Kuroda, 2016). However, limiting its wider use, sales transaction data and view-relevant details are not always (publicly) available, are often limited in geographic coverage, or focus on rare, yet easily extractable view attributes, such as ocean-views (Yamagata et al., 2016). This lack of large scale spatial data hampers efforts to assess the factors that influence visual quality at the building-level, with most studies focusing on a single city or region with sample sizes of typically less than 10,000 observations (Yamagata et al., 2016).

In place of transaction data, income data may be used as a proxy for high quality amenities by modeling income-sorting. Income-sorting can

* Corresponding author.
E-mail addresses: adam.swietek@epfl.ch (A.R. Swietek), marius.zumwald@wuestpartner.com (M. Zumwald).

https://doi.org/10.1016/j.landurbplan.2023.104880
Received 2 February 2023; Received in revised form 23 August 2023; Accepted 1 September 2023
Available online 12 September 2023

be described as the tendency of higher-income earners to settle in regions with better and higher quality amenities (Couture, Gaubert, Handbury, & Hurst, 2023). Lee & Lin 2018 formally extended this theory to natural amenities, presenting evidence that geographic features shape the spatial distribution of incomes. Similarly, Bosker & Buringh, 2017 use geographic attributes to explain initial location choice for European cities, and Burchfield, Overman, Puga, & Turner, 2006 and Saiz, 2010 find geography plays a causal role in a city's continued urban growth and development. Beyond obvious factors, such as waterbodies, other amenities, such as climate and seasonal temperatures have also been found to play an important role in household income sorting (Sinha, Caulkins, & Cropper, 2021). Importantly, terrain hilliness contributes to income-segregation, where the view – as a 'housing luxury good' – likely plays an important, yet difficult to assess role (Ye & Becker, 2018). Despite recent progress, leveraging income sorting to reveal location preference for building-level views remains challenging for different reasons. Although income statistics are typically widely available, they are reported on aggregate as commune, zip-code, or district-level averages. For small scale studies, this leads to an insufficient number of observations for inference. As a result, view attributes can only be assessed if they are either aggregated (based on landscape or urban features rather than building-level information) or they are extracted on a large scale.

To overcome these challenges, we present a large scale approach aimed at establishing a building-level metric for visual landscape quality. The methodology combines income with quantitative view data on a national scale. Based on previous findings that high-quality views are economic determinants of property valuation and of an individual's judgement, attention, and decisions (Ko et al., 2022), we hypothesize that a building's visual landscape quality plays an important role in residential income-sorting. Consequently, average communal income levels should reflect visual preferences. Leveraging this relationship, we characterize the preference for a building's visual landscape by the observed relationship between building-level view metrics and regional income level. To do so, we first derive building-level view-metrics from a 3D digital model of the Swiss building stock, including topography and land use. Next, we model commune-level income as a function of a building's view-metrics using machine learning. Calibrating building-level view metrics with average incomes allows us to derive a single composite measure for each building, namely its visual capital (VC), which can be understood as the scaled predicted income of a household residing in a building with a given portfolio of viewpoints. Large geographic-coverage analysis of VC allows us to reveal spatial patterns of visual inequality, and to define new urban boundaries of similarly ranked visual landscapes. These de novo boundaries of high or low VC could enable future studies interested in socio-economic covariates, such as urban health, within and across income levels. Importantly, we can infer the relative strength of view-driven income-sorting for a given region and relate it to differences in natural and urban form.

2. Literature review

2.1. Spatial feature extraction

The availability of satellite and street-view images has enabled a range of methods to quantify visual attributes of urban areas (Biljecki & Ito, 2021). Although informative on a neighborhood level, such image-based feature-extraction and evaluation methods do not generalize well to views from an individual building (i.e. street-view images can be a proxy for neighborhood appeal, but not for visual landscape differences across neighboring buildings).

To investigate a building's visual landscape, Digital Twins, or simulated 3D urban environments are a common alternative to satellite and street-view imagery. Although qualitatively not as detailed as an image, they capture 3D information from an elevation- and orientation-specific vantage point, thus enabling a more comprehensive and quantitative definition of a view. Information with respect to elevation and orientation provides a greater spatial resolution for viewshed and visibility analysis; as well as for noise, solar and similar environmental simulation common to urban informatics (Biljecki, Stoter, Ledoux, Zlatanova, & Çöltekin, 2015). Further, due to crowdsourcing and federal open data initiatives, 3D urban data have become widely available, enabling urban informatic applications at a large geographic coverage. Highlighting the scalability of 3D data, Milojevic-Dupont et al., 2023 harmonized disparate databases covering the European building stock, and Biljecki & Chow, 2022 consolidated common building morphology metrics and developed a global database. Despite these advantages, country scale studies focusing on building-level environmental performance have been limited to heat demand (Buffat, Froemelt, Heeren, Raubal, & Hellweg, 2017), and roof top solar potential (Assouline, Mohajeri, & Scartezzini, 2017; Walch, Castello, Mohajeri, & Scartezzini, 2020). To our knowledge, there are no previous studies that have quantified visual landscapes from the perspective of individual buildings on a national scale.

This gap in research is in part due to the abstract nature of the view. Unlike other environmental quality attributes such as solar and noise, the extent of possible metrics to describe view quality is considerably broader, making consensus on measurement difficult. As a result, scaling and evaluating the view quality demands greater computational effort. Broadly, we find that 3D-view based metrics define a visual landscape quality by the elements it contains – mountains, greenery, historical buildings, agriculture and similar land use categories (Baranzini & Schaerer, 2011; Yamagata et al., 2016, 2016; Yu et al., 2016), or by the spatial arrangement of elements unique to the observer's perspective – access, distance, sky-openness & diversity (Turan, Chegut, Fink, & Reinhart, 2020; Turan et al., 2021; Yu et al., 2020). Although there are many more possible ways to describe the view-metrics, the categorization given above is in line with the approaches previously utilized in spatial statistics and spatial pattern comparison (Long & Robertson, 2018), namely those that measure the spatial patterns that relate the abundance and arrangement of values. It is thus feasible to characterize a building's visual landscape based on the composition and configuration of elements visible from the set of facade viewpoints associated with the building. Put another way, composition metrics define the aspatial properties of each element within a visual landscape (e.g. view of a lake, sky-view-factor, proportion of views onto greenery)., whereas configuration metrics define the spatial properties of elements within the visual landscape (e.g. balance of all elements, total elements in far distance). The required computation efforts to apply such structured approaches, however, has thus far limited studies to single cities or smaller geographic area, which in turn inhibits a wider adoption and reach across disciplinary boundaries (Inglis et al., 2022; Kang & Liu, 2022; Yamagata et al., 2016).

2.2. Evaluation of view-metrics

Substantial effort has been devoted to determining and correctly quantifying attributes of a 'good view' from an urban and building-level perspective. Yet, there are few empirical studies on landscape preference, and the methods to weigh the importance of visual attributes remain disparate (Inglis et al., 2022; Kang & Liu, 2022). A likely confounder is that what constitutes a 'good view' is complex and driven by both individual and societal preferences. This complexity may not simply be described by the sum of individual elements, but rather by a nonlinear weighting of elements according to their arrangement, proportion, scarcity, cultural importance, and overall context.

Interestingly, although no standardized measure of a building's visual landscape quality exists, window-views and visual quality are commonly understood to play an important role in how individuals perceive landscapes and make decisions (Ko et al., 2022; Schutte & Malouff, 1986; Ulrich, 1977, 1981, 1986). Accounting for visual quality and an individual's preference thereof is thus an important consideration when it comes to financial and urban planning decisions in the context of the built environment. For instance, it is known that visual landscape quality influences public opinion in Switzerland, and increases the economic value of a building (Lindenthal, 2020; Lindenthal & Johnson, 2021; Turan et al., 2021), and changes to the visual landscape have a measurable impact on public perception (Ögçe, Müderrisoğlu, & Uzun, 2020; Oh, 1998). Yet the methods to support these findings rely on disparate sets of spatial metrics that are difficult to compare. Therefore, the creation of a unifying, quantitative measure to represent a building's visual landscape quality would represent an important step forward, facilitating cross disciplinary adaptation (Inglis et al., 2022; Kang & Liu, 2022).

In perhaps the closest adaptation of such goals, Walz et al and Roth et al have introduced methodologies for a country-scale scenic landscape assessment. However, since they had to rely on stated-preference surveys and 2D imagery, the resolution of the produced estimates remained restricted to 1 to 5 km (Roth et al., 2018; Walz & Stein, 2018).

To our knowledge, a structured approach by which to evaluate the weighted importance of elements in the visual landscape of buildings has yet to be developed. Only then can building-specific estimates of visual landscape quality be assessed at a national scale.

3. Data & methods

In the following section we outline the steps to develop a large-scale accounting of Switzerland's building-level visual landscapes and to investigate its variability across urban agglomerations and topology.

3.1. Viewpoint visual share data

Our approach leverages a precomputed dataset containing point-of-view results from a viewshed visibility simulation based on open-access 3D databases, and presents a systematic and automated method to develop building-level view-indicators. Specifically, the large-scale viewpoint visibility analysis and resulting visual share dataset, provided by n-Sphere and Wüest Partner, was computed using a ray-tracing approach, whereby the proportion of rays cast outward, in a 120-degree cone orthogonal to the facade surface (Fig. 1) from a single facade viewpoint, that intersect a select visible element represents the visual share of that element. Visual shares are expressed as a percentage ranging from 0 to 100%, and the total visual share proportions for a single facade viewpoint sum to 100%. A single facade viewpoint observation containing visual share data can be thought of as an image taken from a window. In Fig. 1, we illustrate the data sources and how this procedure was applied to a generated 3D urban environment. Origin viewpoints were computed for all facades and floors within a building, and viewpoint target intersection information, distances between origin and target points, as well as obstructions and landscape elements in line of sight were recorded. Table 1 describes the landscape elements, obstructions, and distances contained within the provided database. The selection of landscape elements is limited to the elements provided in the landcover maps (Federal Office of Topography swisstopo, 2018b) that the view database is derived from.

3.2. Developing building-level view-metrics

As a result of the viewpoint spacing approach used to develop the visual share dataset, the number of viewpoint observations collected per

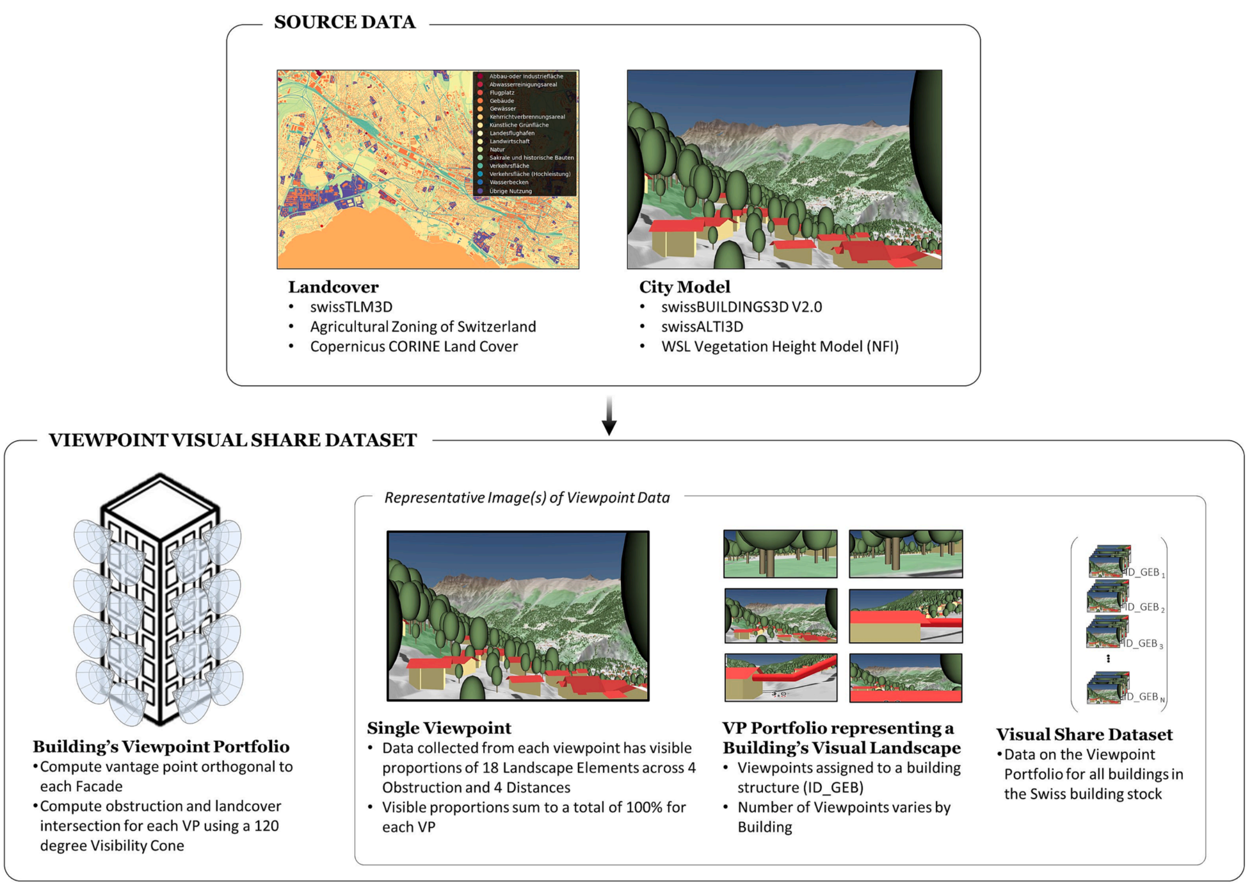

Fig. 1. Schematic summarizing the visual share dataset. Data collected from each Viewpoint (VP) is illustrated with a representative Viewpoint Image. The actual database contains values representing the proportion of each landscape element visible from a single VP.

Table 1
Landscape elements and distance considered.

Visual Element		Distance
Mining and Industrial	National Airport	Near *(< 100 m)*
Waste-Water Treatment	Agriculture	Mid *(100 m – 1 km)*
Roof Obstruction	Nature	Far *(1 km – 50 km)*
Facade Obstruction	Sacred/Historic Buildings	Infinite *(>50 km)*
Airfield	Other	
Buildings	Vegetation Obstruction	
Water Bodies	Traffic area	
Heliport	High-performing Traffic area	
Waste Incineration	Water Basin	
Artificial Green	Sky	

building varies with the size of the building, i.e. the larger the facade surface area, the more viewpoints. Since we are primarily interested in comparing the view quality of one building vs. another, we first generated building-level indicators from the viewpoint visual share data. Specifically, we compute two sets of building-level summary statistics. They characterize the view based on the abundance (composition) and arrangement (configuration) of visible elements, which from hereon are referred to as *visual composition* and *visual configuration*. Building level metrics used in this study are listed in Table 2 with examples for further clarification. Together, the 57 developed visual composition and configuration metrics (see summary statistics in Table 3 Table 4) quantify the quality of the visual landscape. In Fig. 2, we illustrate the main steps in our methodology.

3.2.1. Defining visual composition

Visual composition, defines the visual landscape in terms of individual elements or points of interest. We propose maximum visual share (*maxVSH*) and visual access (*VA*) to represent aggregate values of a single element within a select building (see Table 2).

Table 2
Definitions for visual composition and configuration metrics.

Visual Composition

ID	View-Metric	Description of Calculation
maxVSH	maximum visual share	The maximum visible share of a select element from the set of a building's viewpoints. e.g. out of all visual shares of the lake, the maxVSH for a building may be 5%.
VA	visual access	The fraction of a building's viewpoints that have a visible share that meets a minimum threshold of 1%. e.g. a 1% view of the lake is visible from 10% of a building's viewpoints.

Visual Configuration

ID	**View-Metric**	**Description of Calculation**
richness	element richness	The total number of unique visual elements from a single viewpoint. E.g. 5 landscape elements are visible from a given point.
balance/ gini	element balance	The statistical dispersion of the visual shares of unique elements from a single viewpoint. E.g. 5 unique landscape elements each with a 20% visual share, would produce a perfect equality balance score of 0.
pano	panorama	The total visual share of elements (excluding sky) located in the far and infinite distance, i.e. >1 km away.
refuge	refuge	The ratio between the total visible share of elements in far distance and the near distance. E.g. the visible share of far elements in the distance is 10% that of elements in the near distance.
snt	visual sentiment	The total visual share of positive, negative, or neutral elements from a single viewpoint. E.g. 20% of the visual landscape is attributable to positively labeled elements (vegetation, water, nature, etc.).
dist	visual distance	The total visual share of elements located at a particular distance: Near, Mid, Far, and Infinite distance. 25% of the visual share is of elements in the near distance.

Table 3
Summary Statistics for Visual Composition Indicators for 33 million viewpoints.

ID	*Visual Element*	Visual Composition					
		Max Visual Share (maxVSH)		Mean Visual Share (mnVSH)		Visual Access (VA)	
		mean	*std*	*mean*	*std*	*mean*	*std*
Abb7	Mining and Industrial	0.27	2.63	0.09	1.31	6.26	17.19
Abw14	Waste-Water Treatment	0.05	1.36	0.03	0.82	0.40	4.71
Dac1	Roof Obstruction	6.88	11.47	1.85	3.50	80.84	27.27
Fas2	Facade Obstruction	26.33	21.86	12.99	11.57	91.77	20.08
Flu18	Airfield	0.01	0.66	0.01	0.42	0.49	5.03
Geb12	Buildings	11.94	10.53	3.85	4.04	88.35	20.24
Gew1	Water Bodies	0.34	2.52	0.13	1.20	9.56	21.57
Hel19	Heliport	–	0.19	–	0.12	0.01	0.69
Keh15	Waste Incineration	0.01	0.45	–	0.23	0.06	1.69
Kue8	Artificial Green	33.64	16.88	22.75	12.67	89.21	26.73
Lan10	National Airport	5.19	12.34	3.02	8.75	52.39	39.09
Lan17	Agriculture	0.01	0.69	0.01	0.40	0.38	4.40
Nat3	Nature	7.54	14.12	4.81	10.74	76.19	29.69
Sak13	Sacred/ Historic Buildings	0.10	1.57	0.03	0.58	1.38	7.78
Ueb5	Other	0.60	4.59	0.29	2.62	7.00	18.19
Veg3	Vegetation Obstruction	22.42	16.93	12.62	10.61	97.22	10.62
Ver6	Traffic area	0.16	1.91	0.04	0.60	5.01	15.01
Ver11	High-performing Traffic area	9.68	11.34	3.31	4.47	76.29	28.88
Was16	Water Basin	0.12	1.37	0.03	0.40	2.12	9.37
Sky	Sky	40.94	6.59	34.14	7.19	99.62	3.89

The first visual composition metric, *maxVSH*, describes the maximum visual share of a selected target element (e.g. Nature) from a select building's set of viewpoints. Using the maxima helps to preserve variance across the national sample and, importantly, is robust to the shape and size of a building's footprint and surface. The second, *VA,* describes the proportion of a building's viewpoints that a select element is visible from. Put another way, the *VA* quantifies the potential exposure a select building has to a select visible element.

3.2.2. Defining visual configuration

Visual configuration, the second approach to define view-metrics, defines the visual landscape in terms of the spatial arrangement of these visible elements from a particular viewpoint. In this paper, we apply the commonly used metrics: richness, balance, panorama, refuge, distance, and sentiment (see Table 2 for definitions and examples). A few of these offer a relative measure of the average visual shares (as a %) across all viewpoints within a building, for all cardinal directions (richness, balance, and refuge). The remainder describes a building's average exposure level in terms of distance or sentiment: such as the average sky exposure, or the average exposure to positive elements. Combining these metrics could be particularly useful when comparing the visual landscape from buildings across regions, as each of these measures highlights the spatial structure of elements as opposed to the elements themselves. For instance, element balance informs the degree to which the visual scenery is dominated by a single element or whether an even distribution is present. Similarly, this metric can be repeated to measure the balance of elements grouped by distance. Visual balance as

Table 4
Summary Statistics for Visual Configuration Indicators.

		Visual Configuration						
ID	*View-Metric*	*mean*	*std*	min	*0.25*	*0.50*	*0.75*	max
cmpx_rh	Element Richness	9.42	1.73	1.00	9.00	9.00	10.00	19.00
cmpx_shanon	Element Balance – shanon	1.48	0.18	0.00	1.39	1.50	1.60	2.14
cmpx_gini	Element Balance – gini	0.83	0.03	0.67	0.82	0.83	0.85	0.95
snt_0	Neutral Sentiment	46.94	6.53	0.00	43.25	47.80	50.62	100.0
snt_Neg	Negative Sentiment	3.78	5.42	0.00	0.18	1.69	5.37	91.50
snt_Pos	Positive Sentiment	30.76	10.04	0.00	25.10	31.53	37.30	100.0
rh_snt_0	Neutral Sentiment Richness	7.33	1.82	0.00	6.00	8.00	9.00	12.00
dist_gini	Distance Balance – gini	0.54	0.06	0.07	0.51	0.54	0.57	0.75
pano_sum	Panoramic Share	3.61	4.13	0.00	0.78	2.09	4.97	51.30
pano_rh	Panoramic Richness	22.24	9.94	0.00	15.00	23.00	29.00	85.00
refuge	Refuge	0.64	0.22	0.00	0.50	0.64	0.76	47.66
ShNah1	Share of Elements in Near Distance	62.24	8.49	2.06	56.78	61.10	66.60	100.0
ShMit2	Share of Elements in Mid Distance	2.11	2.61	0.00	0.47	1.22	2.74	46.84
ShFer3	Share of Elements in Far Distance	1.50	2.36	0.00	0.09	0.46	1.87	37.22
ShUne4	Share of Elements in Inf Distance	0.01	0.02	0.00	0.00	0.00	0.00	1.33
ShSky	Share of Sky	34.14	7.19	0.00	30.42	35.38	39.25	50.62

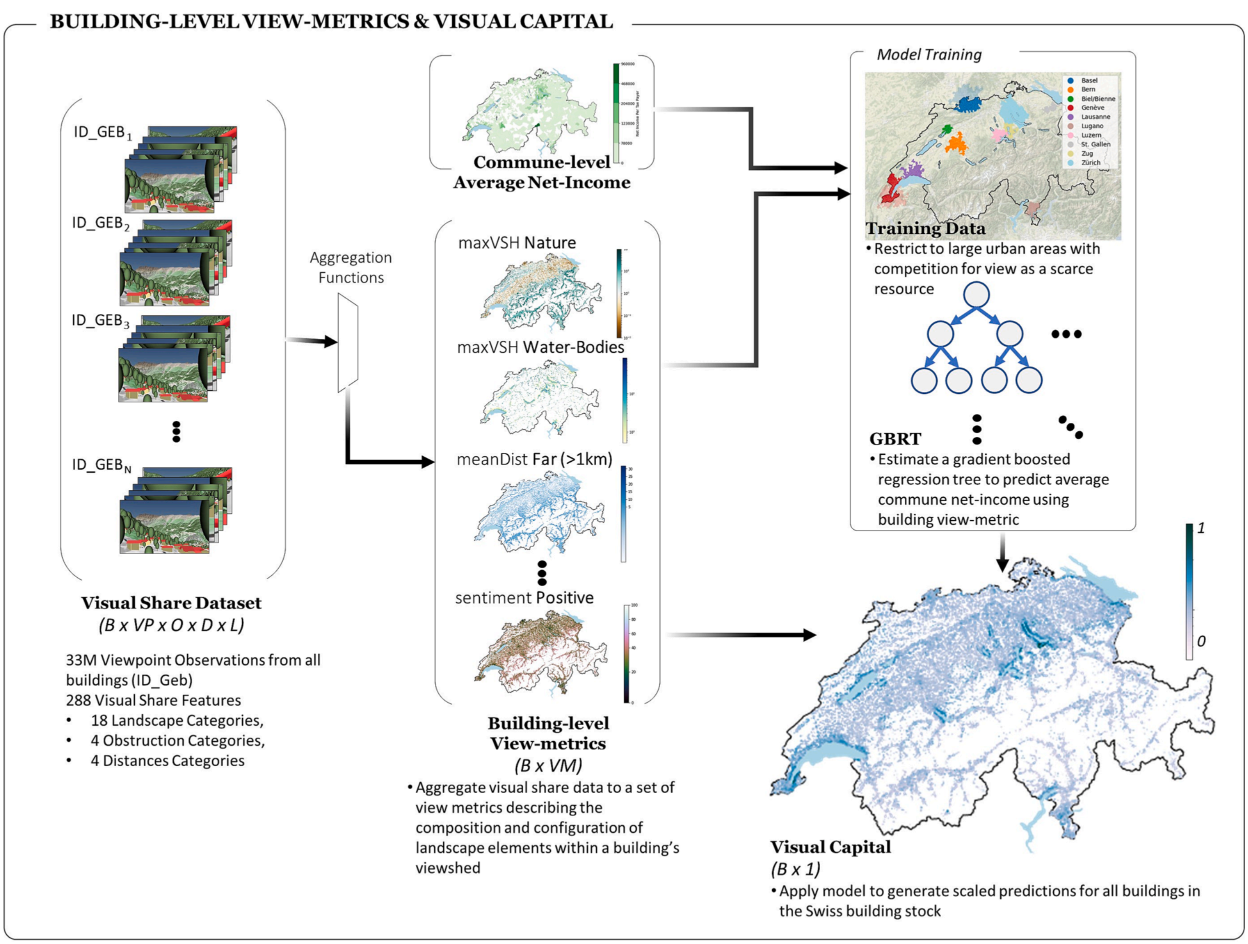

Fig. 2. Schematic summarizing the developed methodology.

a function of distance could help to characterize the natural topography (e.g. terrain slope) and the urban form, e.g. dense urban core, suburban periphery, or rural outskirts.

3.3. Measuring visual capital

To perform a national-scale evaluation and accounting of visual landscapes and of window-views, we develop a framework to measure VC. The measurement framework consists of our 57 view metrics and our target variable, commune-level income (CLI). CLI is assigned using the 2018 average net-income per taxpayer for a given commune (Federal Statistical Office, 2022). We apply a machine learning model that learns the relationship between the two at the building level, granting us a method to directly estimate income from view-data. Specifically, we estimate a gradient-boosted regression tree, eXtreme Gradient Boosting (Chen & Guestrin, 2016). Despite the CLI not varying at the commune level, the large amount of data allows us to extract intra-communal variation across communal building stocks, which enables building-level predictions of CLI, that can solely be attributed to visual characteristics. Hence, while the response variable CLI is uniform across buildings within a commune, the model predictions are individualized. We define the rescaled predictions of a building's 'income' derived directly from the building's view metrics as visual capital (VC).

VC is thus a weighted combination of the visual composition and visual configuration view-metrics that were extracted directly from 3D data of the building itself and its surrounding landscape. Following our assumption that buildings found in high-income neighborhoods have, on average, desirable, high-quality views, our model thus finds the combination of these view-metrics that best predicts CLI. Considering the likely nonlinear nature of visual preference, we use a gradient boosted decision-tree algorithm, which is well suited and has been deployed in similar frameworks, such as predicting an individual's economic success (income) based on friendship network attributes (Chetty et al., 2022). To ensure a high degree of income-sorting (competition for housing), which is generally the case in urban areas, we compile a training sample of buildings located within the top 10 agglomerations (for information on selected agglomerations, see Table 5); located in communes with at least 100 taxpayers; and which have a maximum of five stories. Limiting building height reduces the model's propensity to overfit to inner-city urban areas and minimizes biases that arise due to the underlying correlation of building height and visual composition (e.g. the size of a lake view increases the higher up you are in the same building). The focus of this study is thus on individual and single-family homes, which are typically the main focus of real estate valuation approaches. Our final training sample consists of 781,220 buildings from 365 communes.

3.3.1. Machine learning setup and evaluation

To assess model robustness, we ran 100 iterations of 10-fold spatial cross-validation (see illustration in Supplement Fig. S1A). Each round consists of the following 4 steps: (1) Randomize the order of communes and partition into 10-groups, (2) Train the model on buildings located within communes of 9 groups, (3) Evaluate the model on buildings in the excluded group, assign R^2-score, and (4) Repeat until all 10 groups are excluded. R^2-scores are derived from comparing the average building-level prediction within a commune to that of the average commune-level net income. As a result of the 100 iterations of the 10-fold spatial cross validation, we obtain 1000 models, where each commune has exactly 100 associated R^2-scores. The distribution of model performance provides an assessment and range of how well the model performs and allows us to explore communes associated with under/over performing models. After validating model robustness, a final model was fit on the entire training dataset. In section 2.5 we further validate our approach by using a separate data-set that provides a high-income label for each commune from the year 2000 (Federal Statistical Office, 2000).

To further assess prediction sensitivity, we compared the results across 7 machine learning regression models: Linear, Penalized Linear Regression (Lasso), Generalized Linear Model (GLM), Light Gradient Boost Model (LightGBM), Neural Network (NN100), Random Forest (RF), and, our chosen model, eXtreme Gradient Boosting (XGB) (Breiman, 2001; Chen & Guestrin, 2016; Ke et al., 2017). In addition to comparing model accuracy on a common test-set, we visually compare the spatial distribution of fitted valuation for lake-shore communes with 3 different CLIs: Morges (CHF 79 K), Préverenges (CHF 96 k), and St. Sulpice (CHF 134 k). This helps to visually determine whether the model is simply learning administrative boundaries or rather important visual characteristic. Lastly, we compare the correlation of the fitted values to the individual view-metrics as well as a subset of relevant non-view metrics, to gauge variability of the association between metrics and model predictions. The subset of used non-view metrics define building attributes (including year of construction, volume, land area, condition, free-standing, number of rooms, sun exposure, street noise), distances to regional amenities (including main street, train station, atomic power plant, city center, shopping, nature, lake, river, and public transport) and location attributes (including lake access, and public transport quality).

To better interpret the influence of a select view-metric, we implement the SHAP algorithm, which quantifies the optimal credit allocation across all model features (Lundberg & Lee, 2017) and computes a proxy value characterizing the marginal contribution of each feature towards one additional unit of VC. The SHAP algorithm provides greater model explainability, and as a result has become common place in spatial modeling methodologies. For example, a recent study (Zekar, Milojevic-Dupont, Zumwald, Wagner, & Creutzig, 2023) used the method to measure the effect of urban form features on temperature changes. Additionally, SHAP allows us to explore the context-dependence of view-metrics. After training the final model, we rescale the fitted values to derive the normalized [0,1] measure of VC across the entire building stock sample. For spatial analysis, we can further standardize these values, centering the mean at 0, to visually identify regions that tend to be above or below average.

3.4. Measuring regional difference of visual capital

Building level indicators at a national-scale enable a quantitative assessment of inter- and intra-regional differences. In this study we summarize a region by the median building value or the proportion of buildings with a select value; for instance, the percentage of buildings in a commune with a *maxVSH*>1%. When directly comparing the distributions of building-level values across regions or agglomerations, we additionally account for spatial concentrations of buildings. To do so, we can group buildings into 1-km^2 regions, called hexbins. Such standardized hexbin regions control for the spatial dispersion of buildings and allow to directly compare the spatial distribution of a value across an agglomeration. When comparing landscape topology differences across regions, utilizing administrative boundaries such as communes can

Table 5
Summary of commune-level income statistics for agglomerations used in training sample.

Agglomeration	No. Communes	No. Buildings	Commune Average Net-income Per Taxpayer (2018, CHF 1′000)					Commune Average Taxable Income Per Tax Payer (2018, CHF 1′000)				
			mean	std	min	median	max	mean	std	min	median	max
Basel	44	92,789	95	16	71	91	135	86	15	64	83	126
Bern	28	62,172	83	10	70	80	121	76	10	64	73	113
Biel/Bienne	11	14,791	75	12	67	69	111	68	11	61	63	102
Geneva	46	62,246	137	62	75	119	480	128	62	67	108	468
Lausanne	35	41,750	99	21	68	92	142	90	20	60	83	133
Lugano	36	43,809	91	16	61	94	146	84	16	56	84	138
Luzern	15	33,411	96	29	67	80	170	88	29	60	74	163
St. Gallen	12	36,025	81	14	70	73	122	74	14	64	67	111
Zug	13	22,952	134	31	78	116	196	126	31	70	108	188
Zurich	106	214,258	108	43	69	92	300	99	43	61	86	292

complicate the analysis, since communes can vary in both size and shape and hence obscure intra-commune variability of the urban and natural form. Thus, in this study, we also calculate a 100 m buffer area for each building and compute the building density (e.g. the number of buildings) and the terrain slope (e.g. the average terrain slope). These buffer areas represent the respective urban and natural forms each building is exposed to. Terrain slope was calculated utilizing readily available digital elevation models of Switzerland (Federal Office of Topography swisstopo, 2018a).

3.5. Drawing new geographic boundaries of high visual capital

To validate and show the usefulness of a building-level measure of VC, we define new geographic boundaries of high-VC as a case-study. Specifically, we adopt the LISA (local indicator of spatial association) method (Anselin, 1995) to isolate buildings that have a spatial association with high values of VC, and partition these buildings into distinct clusters to draw new urban boundaries.

Following the LISA method, we compare the VC of a select building to that of its 100 closest spatially lagged neighbors. To test for the spatial dependence between a building's VC and that of its neighbor, we compute the Local Moran statistic for the observed data and compare it to the Local Moran of a randomly generated set of neighbors. After correcting for multiple hypothesis testing, we retain only the buildings with a significant Local Moran statistic, a high-VC and high spatially lagged-VC. We then group the location (coordinates) of these buildings into distinct clusters using an unsupervised hierarchical density-based clustering method, (HDBscan) (McInnes, Healy, & Astels, 2017). Buildings that are either isolated or in low density areas are considered noise and thus removed. Next, we generate geographic boundaries by calculating the alpha shape for each cluster's set of buildings using an alpha parameter of 0.01. The newly generated shape boundaries are considered regions of high-VC. Note, this process can also be used to identify geographic boundaries of low-visual capital clusters. Importantly, these newly defined boundaries of high VC can be compared against a validation dataset of high-income communes held out of the training sample.

4. Results

4.1. Distribution of building-level view-metrics across the Swiss building stock

We find that the 20 visual elements considered in this study vary in abundance. Fig. 3 shows that only about 15% of the building stock has any view of Water Bodies. Visually abundant elements, such as Nature, Sky and Agriculture, are seen by at least 50% of the building stock (we consider > 0% *maxVSH* as the cutoff for being seen).

While visually-abundant elements exist in similar quantities from region to region, we identify a few exceptions. Buildings in rural regions have about ten times larger view-shares of nature – where a 75th percentile-ranked building in the rural region will have a 10% *maxVSH* of nature, whereas an equally ranked building found in any major agglomeration will have less than a 1% *maxVSH*. For views of vegetation, Geneva ranks highest among Swiss agglomerations, where the median building has a 5–10% greater share. See Supplementary Fig S2, S3,S4 for information on the visually-abundant elements.

Upon inspecting the visually scarce elements, i.e. seen by less than 50% of the building stock, we find much greater variety across the major agglomerations of Switzerland (see Supplementary Fig. S2). Buildings in Lausanne are more likely to have a view onto a body of water, with 40% of buildings having a water-view of some quantity; approximately 15% more than in Zurich and 30% more than in Bern and Basel (river-cities). We find substantial differences in visual configuration across urban and landscape typology classification (see Supplementary Fig. S3, S4). For example, visual landscape for urban areas is dominated by elements in

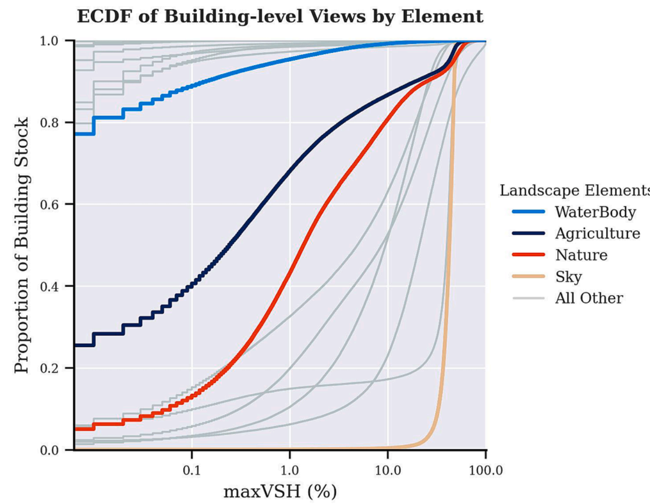

Fig. 3. ECDF of maxVSH elements across the Swiss building stock. Figure indicates that building-level views of elements vary in abundance, where abundant elements are seen (maxvsh >0%) by more than half of the building stock and scarce elements are visible in less than half.

the near distance, whereas the Alpine region boasts more balanced views and has the largest panoramic views, namely 4 to 8-fold larger than other terrain typologies.

4.2. Model

4.2.1. Model results

We assess the performance of the full XGB model, trained on the full training dataset (i.e. all buildings located within the top 10 agglomerations), by comparing the average model prediction across all buildings within a commune to the commune's actual average net-income per taxpayer – the CLI. We find that the residuals for average commune predictions are normally distributed for communes with a CLI of less than or equal to CHF 100 k, whereas for communes above this threshold the residuals are skewed and the 95% percentile ranked prediction is a better predictor of CLI than the mean predicted value (Fig. 4).

The k-fold spatial cross validation procedure (section 2.4) confirms the robustness of the chosen XGB methodology, with a normally

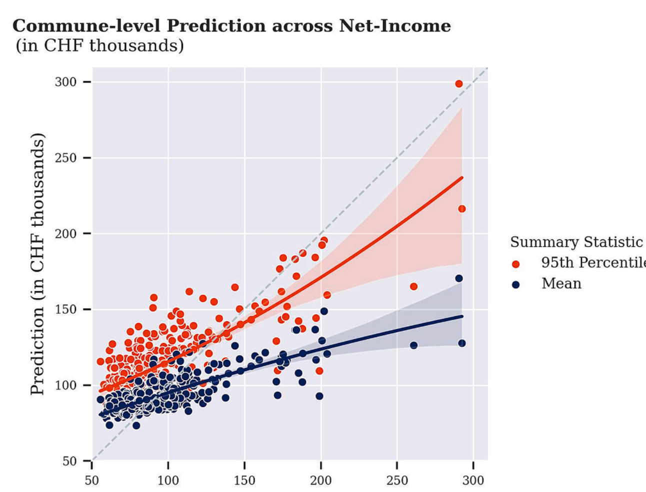

Fig. 4. Scatterplot of commune-level predictions against commune-level net-income. Plot illustrates the dispersion of commune-level prediction increases against net-income, where the 95th percentile and Mean score are shown in Red and Blue.

distributed model performance (mean of R^2-score = 0.32, standard deviation = 0.09) consistent across agglomerations (see Supplementary Fig S1). The final model achieved an R^2-score of 0.47, which falls within the upper decile of the cross-validation performance range (see Supplement Fig. S1).

We find model estimates are robust to other tested regression architectures: Linear, Lasso, GLM, LightGBM, NN100, XGBoost, and RF regression models (see Supplementary Fig. S5). Specifically, the individual correlation of each model's prediction against individual view-metrics is consistent across all models (see Supplementary Fig. S5A). While correlations between model predictions and the subsets of non-view metrics are equally consistent; values for non-linear model architectures (LGBM, XGB, NN100, and RF) are more similar than for linear architectures (Linear, Lasso, GLM) (see Supplementary Fig. S5B). While the Random Forest model maintained similar prediction accuracy compared to the two gradient boosted regression tree models (i.e. LGBM and XGB), it was prone to overfit to the training data and the compute time was orders of magnitudes larger (see Supplementary Fig S6) than the XGB model, chosen in this study.

4.2.2. *Understanding the factors that determine visual capital*

We find that a handful of metrics have a particularly strong positive impact on the model prediction (Fig. 5A and Supplementary Fig S7). Greater visible proportions (i.e. *maxVSH)* of water-bodies, sky and far-distance views contribute positively while agriculture views are inversely predictive of high CLI and indicate distinct non-linear effects. Importantly, we find the influence of most landscape elements on model prediction is context-dependent, i.e., conditional on the other elements within the same visual landscape (Fig. 5B-E). For example, the influence of a nature view varies with the visual access to waterbodies (Fig. 5B), and large (50% or greater maxVSH) views of vegetation are amplified in the context of an imbalanced share of elements and a balanced proportion of the visible distances; i.e. elements in the near, mid, far, infinite distance (Fig. 5E). Views of waterbodies have a substantial influence on the prediction, and can amplify the influence of views of elements in the far distance (Fig. 5D). Interestingly, sky exposure has a persistent influence on the predictive capacity of all other attributes. For instance, within the context of limited sky exposure, views of buildings have a negative impact on predictions. Conversely, views of buildings with high sky exposure positively influence the predictions (Fig. 5C).

4.3. *Visual capital*

In the following section, we present Visual Capital (VC), the rescaled fitted values representing the building-level visual landscape quality preference across the entire swiss building stock. We directly compare the VC of cities and communes and present evidence illustrating (1) the extent to which visual quality contributes to income sorting within and across agglomerations, (2) VC's association to the urban and natural form, and (3) a validation case-study that correctly identifies held-out high-income regions.

4.3.1. *Regional difference in visual capital*

Generally, we find that averaging all building level VC predictions per commune correlates well with the CLI of the respective commune, however, in some Swiss cities this relationship is stronger than in others. Comparing Lausanne and Basel, which are two cities with a similar CLI range, we find that view metrics are more predictive of CLI in Lausanne than Basel, suggesting that view-based income sorting is stronger in Lausanne, whereas in Basel other socio-economic factors may play a more important role (Fig. 6). Comparing the slopes across the top ten agglomerations, we can identify Zug and Lausanne as the cities with the strongest slope, i.e. VC to CLI association.

Another indicator we can compare across agglomerations is average predicted VC. Conceptually this can be understood as the expected view when choosing a building at random. We find that Geneva and Lausanne achieve the highest average VC. Importantly this is true even in the lowest CLI bins, indicated by a higher intercept for the agglomeration-specific fitted line in Fig. 6. Zurich, although situated by a lake, barely ranks higher than river-cities like Basel and Bern. Beyond average expectations, the variability in building-level predictions of VC for a given income bin allows us to investigate "view-inequality" both at a global and local scale.

4.3.2. *Generalizing the regional difference in visual capital*

To investigate what drives the differences in the average and the variability of VC across different agglomerations, we analyzed the spatial distribution of VC across agglomerations. We observe a similar spatial dispersion of VC in Lausanne and Geneva; whereas Zug and Zurich exhibit heavily skewed values. Specifically, the first 60% of Zurich's building-level VC values and land-level values (i.e. using hexbin aggregation to control for spatial dispersion) are substantially lower than that of cities along Lake Geneva (see Supplementary Fig S8). Further, we observe a spatial concentration of high VC along the East and South-Coast of lake Zurich; whereas in Lausanne VC is evenly distributed across the city boundaries. Fig. 7 illustrates the spatial distribution of above average VC and highlights the importance of distance to lakes for all cities. Intriguingly, the spatial distribution of VC across the two cities Zurich and Lausanne appears to not only reflect distance to the body of water (see Supplementary Fig S9), but also differences in natural topography. For instance, Lausanne sits on a hill, however, its downtown lies in an area of depression, which is reflected by lower VC

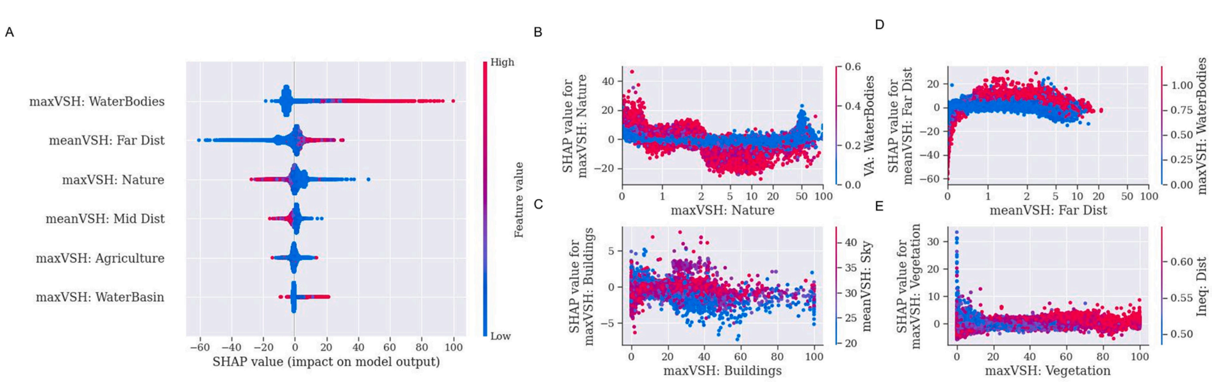

Fig. 5. Impact of view-metrics on a single building's prediction. (A) Summary plot illustrates the SHAP value of a single instance and directionality of impact of the view-metric, where high and low feature values are shown in Red and Blue. The impact of the top 6 features are shown, the remaining, less influential metrics (by absolute mean) can be found in the Supplementary material Fig S7. Interaction plots show that prediction influence of (B) nature views vary across visual access to water, (C) views of buildings vary against sky exposure, (D) larger views of a waterbodies in the same scenery, as well as views of far-distance, have larger predictions than smaller views of waterbodies, and (E) vegetation varies across distance inequality.

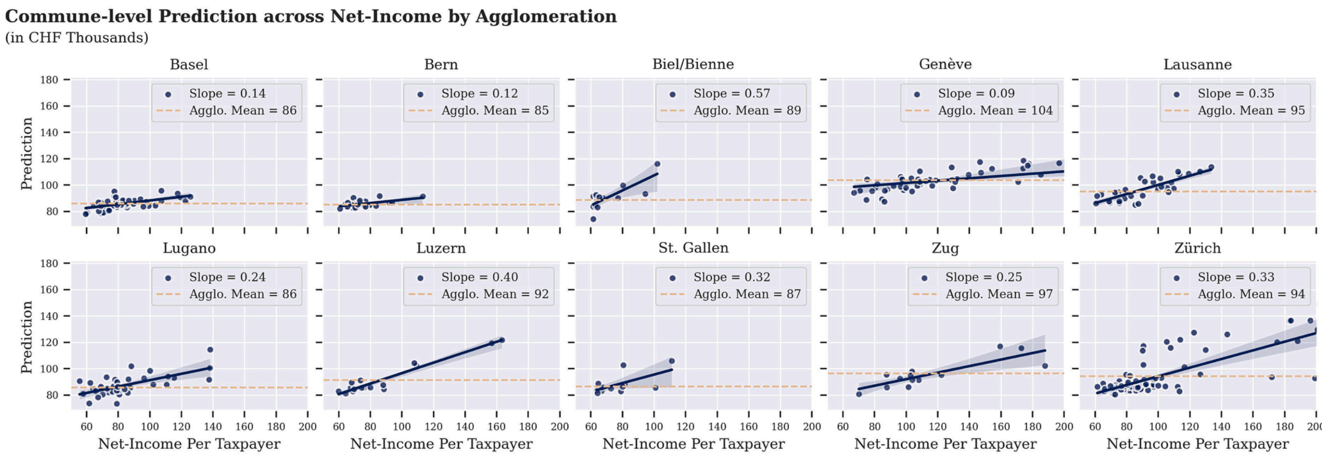

Fig. 6. Scatterplot of Commune-level prediction for the 10 largest Swiss urban agglomerations. A fitted line, and it's slope shown in blue and the agglomeration's mean prediction is shown in orange. The plot and computed slope describe the degree to which income sorting can explain residential sorting variations across Switzerland. A steeper slope, e.g. Lausanne, implies that the visual environment can describe the difference between low- and high-income communes; whereas in Bern smaller differences in visual capital between the high- and low- income communes, i.e. flatter slopes, suggests visual landscape to be less important to the residential income sorting process.

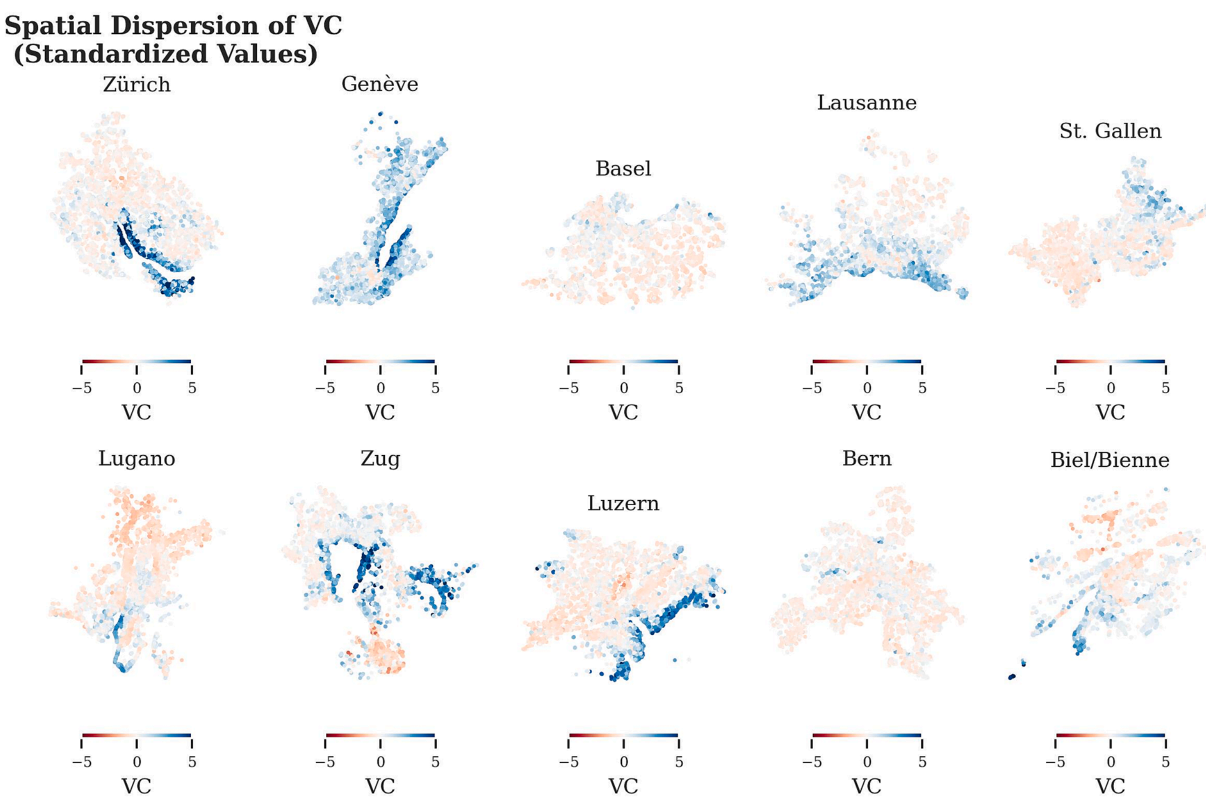

Fig. 7. Spatial Distribution of Visual Capital across Swiss agglomerations. Standardized VC values are used to illustrate the spatial dispersion of above and below average within and across agglomerations.

values for buildings in this area (Fig. 7). Similar holds true for the nine other agglomerations. This indicates that our measure of VC can accurately capture natural form.

4.3.3. *Visual capital and the urban natural form*

At the national scale, we observe that buildings with high visual-capital tend to be located near lakes and on the foothills of the Alps (Fig. 8). As such, our building-level view scores confirm what one might expect, that rural-like views are most sought after when buildings are located within urban centers. The concentration of popular urban view-preferences at the foothill of the Alps further suggests that there may be a direct link between VC and landscape topography such as hilly/mountainous terrains. Supporting this notion, intra-communal variation in VC still display spatial patterns, with similar VC values forming localized clusters (Fig. 8).

When we stratify VC by landscape attributes (the slope of the land the buildings are located on) and the urban form (using building density within 100 m as a representation), a non-linear pattern emerges. It recapitulates the intuition one might have on the relationship across terrain slope, building density and views: the average VC of dense urban

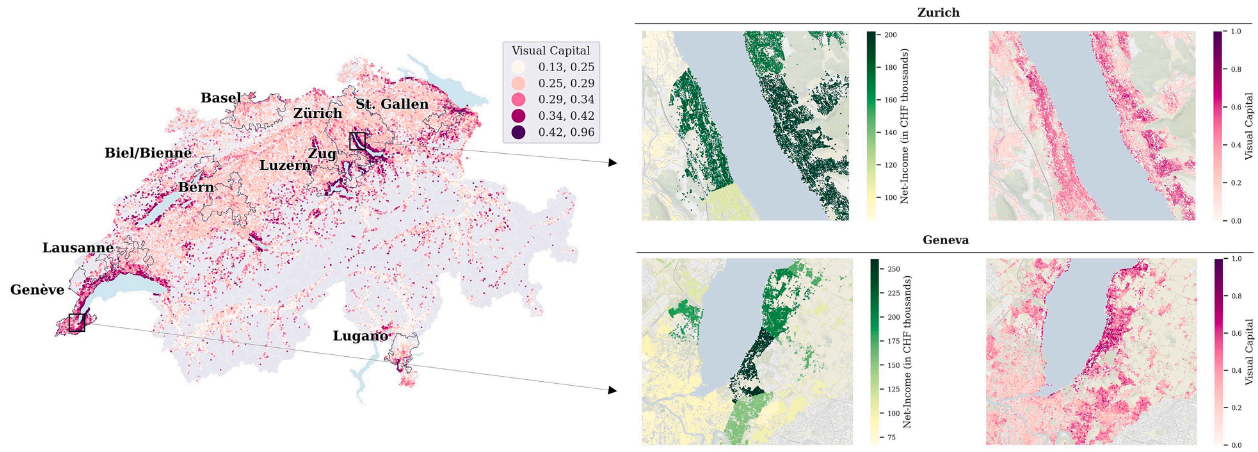

Fig. 8. Choropleth depicting visual capital of the Swiss building stock shows higher levels of visual capital are found nearby lakes and on the foothills of the Alps. Comparison of the distribution of building-level average net-income and Visual Capital values for Zurich and Geneva reveals that VC captures intra-communal differences in building-level view quality.

areas increases with the slope of the terrain, as steeper slopes make it more likely that the view of a given building is not obstructed by another one (Fig. 9). Unlike income, the optimal VC trendline cannot be defined to a single best slope, as lower density areas can achieve similarly good or better views with minimal elevation gain. Moreover, the likelihood of a good view decreases once the slope of the terrain passes 20%, which may indicate distance from other important urban view indicators, such as view complexity. Further, investigating the VC variance within a given urban and natural form bin, confirms that VC scores reflect our intuitive understanding of the relationship between view and the urban form: For low-density urban environments, the skewness of visual capital remains low across terrain slopes, as buildings are spread out making it less likely that one building's view is influenced by another; on the contrary, skewness increases for dense regions as a function of terrain slope, with a hotspot of high-VC skewness within dense urban areas with a moderately steep elevation gain, indicative of visual obstruction due to neighboring buildings as a driver for view inequality (Fig. 9). This presents strong evidence that our model of building-level VC accurately reflects important view characteristics, such as the intricate interplay between typology, terrain, and building-specific viewpoints that cannot be captured by a simple measure such as CLI (Supplementary Fig S10).

4.3.4. *Drawing geographic boundaries of high Visual-Capital*

Here we present the result from our methodology to generate micro-location visual quality indicators for our validation case study in Lausanne. We group buildings based on their VC similarity and identify natural boundaries of shared visual quality.

Our spatial clustering analysis of Lausanne identifies a number of high-VC clusters (Fig. 10). The generated regions overlap, to a large extent, with both administrative boundaries of high-income communes used during the model training, as well as those held-out for testing. However, our newly defined regions often extend past these predefined administrative bounds. This spill-over effect tends to track with terrain and urban form, confirming our previous findings. For example, Fig. 10 shows the largest identified cluster encompasses the majority of the commune Pully, which has an average CLI of CHF 119 k, however, the natural view boundaries spill over into the neighboring commune of Lausanne center, whose CLI is a comparatively meager CHF 79 k. We identify high VC spill-over in several other high-income communes, such as Saint-Sulpice, Buchillon, and Saint-Prex. Notably, despite being surrounded by lower-income communes, a cluster of high VC is found within the boundary of Jouxtens-Mezery, whose net-income per taxpayer information was not publicly available, however gross net-income data from 2018 and tax data from the year 2000 labeled this commune as high-income (Fig. 10). Furthermore, we identify several smaller clusters of high VC that are not labeled as high income, either because of missing data or because they are located in lower income communes. These findings indicate that spatial clustering of VC can serve as a local indicator of areas with similar, and particularly highly valued views. This analysis may be extended to locate clusters of low-VC

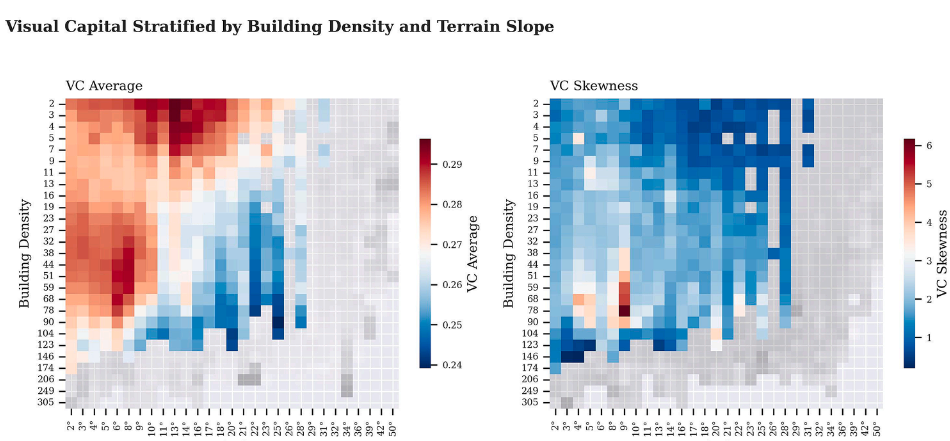

Fig. 9. Heatmap depicts the average VC (left) and skewness of VC (right) when stratified by urban and natural form; i.e. building density (100 m radius) and terrain slope (1 km area). Urban/Natural form conditions with less than 1000 buildings are excluded (greyed).

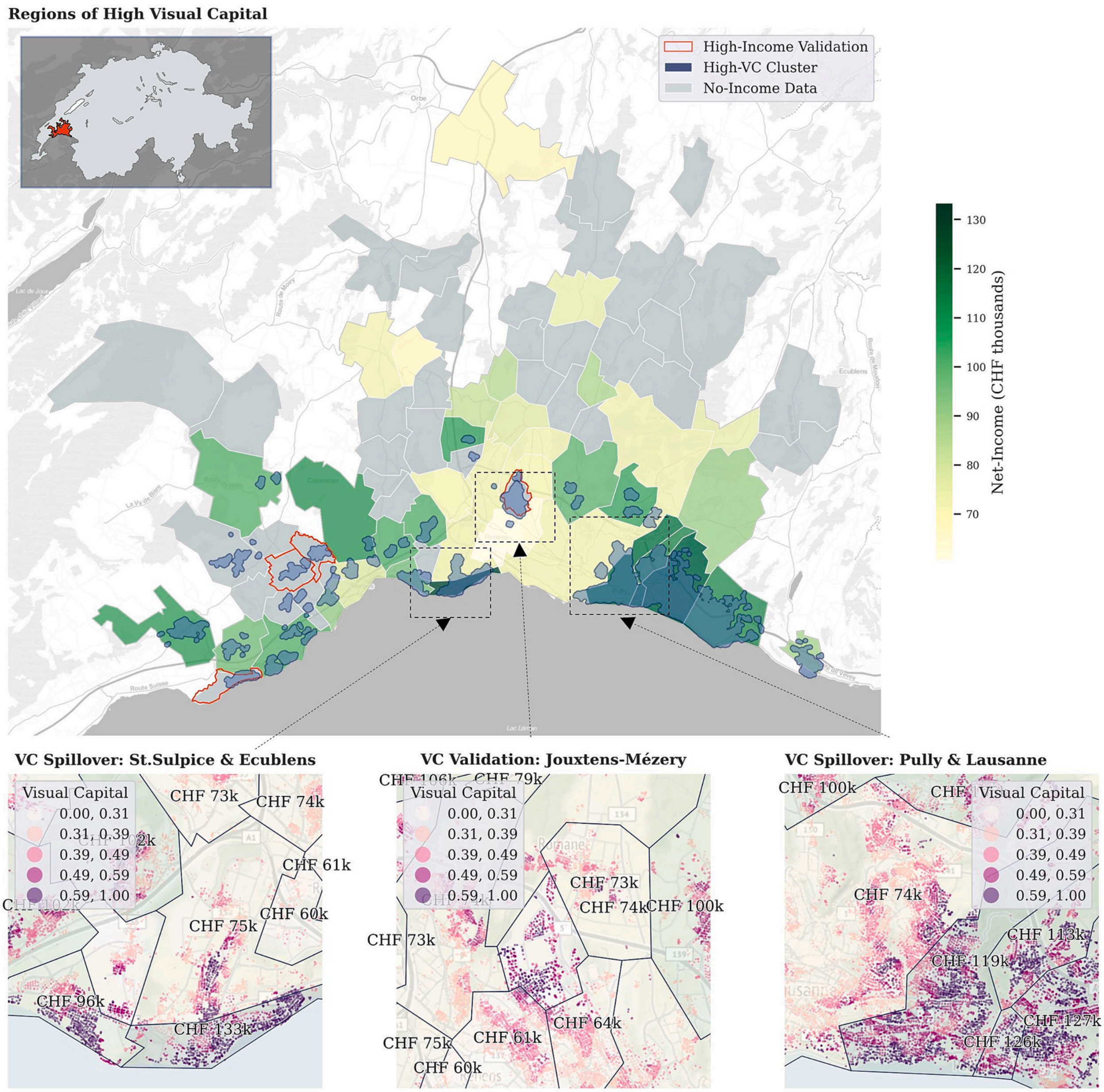

Fig. 10. Computed boundaries of high visual capital (HVC) are shown in blue. Communes with darker shades of green indicate higher income levels, grey communes were excluded from the training-sample because no income data was readily available, and the red border indicates high-income communes as labeled by a secondary data source. HVC appears in all held-out validation samples; including Jouxtens-Mezery. HVC spills past administrative boundaries of high-income neighborhood, including St.Sulpice and Pully.

regions, or be applied to other cities and regions.

5. Discussion

Determining the value of visual landscapes is challenging in part due to the difficulty of how to best quantify the view itself. Viewpoint data from 3D GIS and Digital Twins, in combination with spatial machine-learning techniques, offer an opportunity to both develop comprehensive view-metrics and uncover the context of visual landscape preferences. We leverage commune-level income (CLI) statistics to generate a composite measure of building-level visual landscape quality, which we term visual capital (VC). Visual capital is derived by extracting visual composition and configuration metrics directly from a building's 3D configuration and that of its surrounding environment. Hence, we extend the existing literature in two ways: First, we provide an accounting of the visual landscape of the entire Swiss building stock and, second, we provide a building-level visual landscape ranking in the form of VC, which can be understood as the view-based, individualized 'income' of each building. Furthermore, we show that VC captures non-linear relationships of individual view metrics, urban density and natural form, thus providing an accessible summary indicator of a building's visual environment. Such assessments have remained challenging in the past, due to either a lack of large-scale data or accessible response variables.

Our model relies on the assumption of view-based income sorting, and thus relies on competition for the scarce resource 'good view'. In contrast to previous studies (Inglis et al., 2022), we are not bound by a limited number of observations, thus allowing us to benchmark landscape-based preferences at the resolution of individual buildings. By restricting the trained model to the ten most populous agglomerations, we maximize amenity-driven income sorting effects, providing a more accurate depiction of building-level view preferences. Supporting this notion, view-based income sorting is strongest in agglomerations with access to high-quality views, as typically found in lake-regions. Individualizing view preferences at the building-level in this manner, allows us to quantify and compare how good of a view an average citizen of a select city can expect and what income is required to obtain it.

An important aspect of our approach is the applicability of the learned visual preferences to the entire national building stock, including rural regions. The positive correlation between the variability in inter-commune VC and CLI suggests that communes attracting higher income individuals have larger visual inequality, with only a portion of buildings (20–40%) attaining desirable and differentiable visual landscapes, whereas the VC of the remaining stock resembles that of lower-income communes. Further, we can use the global predictions of VC to assess how the visual landscape quality of Switzerland is associated with both urban and natural form factors. For example, we can confirm the intuitive assertion that, on average, income-sorting tends to favor either elevated or less-dense areas within an agglomeration. Unlike previous studies that lacked building-level information, our methodology reveals a more complex relationship between slope and building-density. The high overall high skewness of VC within dense communes supports that view preferences are well-captured as, unavoidably, there will be buildings whose view remains blocked by others. It further indicates that proximity-metrics (such as distance to the lake) or simple neighborhood-scale attributes, i.e. net-income, may not be sufficient to capture a 'good view' for individual buildings, as it discounts important 3D differentiators such as natural and urban form.

Since the resulting predictions of VC are individualized and thus no longer bound by communal statistics, we can de novo assign 'view-boundaries' that indicate local clusters of buildings with similar VC. These newly defined regions of shared VC may thus provide a basis for view-based micro-location indicators, as commonly used in housing price evaluation studies: comparing clusters of shared VC could highlight buildings or neighborhoods that are over/undervalued with respect to their visual quality. Such assessment could prove valuable to developers looking for properties in economically undervalued, but perhaps visually appealing areas, as well as urban planners interested in quantifying the visual impact of a proposed new development.

A single quantitative measure for building-level VC may provide further benefits: automated real estate valuation and mass-appraisal methods can particularly benefit from building-level differentiation of visual quality. Previous studies have highlighted that iBuyers, who use automated valuation models, are challenged by adverse selection (Buchak, Matvos, Piskorski, & Seru, 2020), which may partly reflect a lack of data on 'hard-to-measure' qualities such as the view. Including VC into valuation models may thus improve the predictive performance of a statistical model. In this context, extending our analysis to individual floors, sides, or even units within a select building, may allow modeling view-based price variation within large multifamily buildings. Further, extending the analysis to focus on other urban form typologies, i.e. tourist communities, may yield interesting insight into the factors that predict visual capital in specific regions or contexts. Pricing studies incorporating sales, rental or hotel prices, while controlling for other important building and local attributes, could further validate the importance of this metric. In addition to determining the willingness to pay with hedonic pricing, studies can utilize mixed-effects models and spatially varying coefficient models (Dambon, Sigrist, & Furrer, 2021) to assess whether the marginal effect of visual capital on home prices varies across space (e.g. coordinates or urban typologies), and income (i.e. as a luxury or inferior good).

Although our building-level VC metric captures many intuitive concepts on how individual view metrics, as well as urban and natural forms, should interact to create a preferential visual landscape, there are several limitations of our automated assessment tool. While it could be reasonable to assume that visual landscape preferences do not significantly change from year to year, our approach only considers income from a single year and thus may not fully represent changes in visual preferences over time. Despite defining view-metrics at nation-wide resolution, the view-metrics used in this study cannot fully capture the aesthetic quality of a particular view. For example, we currently cannot differentiate the view towards a facade with damaged and unmaintained cladding from one with architectural sculptures and intricate stonework. Thus visual capital may struggle to explain income sorting for building stocks with undifferentiable visual landscapes or with variability arising from a more abstract level of detail, such as specific building components. Future approaches may thus benefit from incorporating aesthetic aspects, i.e. as learned from street view images.

Lastly, our approach is restricted to buildings for which 3D GIS models are available. With more regions and countries digitizing their building stock, and given the standardized approach to generate view metrics, it should however become feasible to extend our analysis and compare differences in view preferences across a more diverse building stock. Comparing results from two or more regions with differing source 3D data may require additional data engineering to ensure reliability of results and consistency of labeling.

6. Conclusion

Evaluating visual landscape quality at large-scale has remained challenging. In this paper we have introduced a spatial machine learning approach to generate an income-derived building-specific measure of Visual Capital.

We identify that waterbodies, elements in the distance (>1km), and sky exposure are the strongest individual predictors of high-income. We further show a context-dependency of individual view metrics, with certain features gaining importance only in the presence of another.

We demonstrate the utility of this approach by estimating Visual Capital values for the entire Swiss building stock and investigating the inter- and intra-regional distribution in building-level Visual Capital, including view equity, and the agglomeration-specific degree to which view contributes to income-sorting. We further show that our composite measure of Visual Capital captures urban and natural form attributes, such as a non-linear relationship of view quality with terrain slope and building density. Lastly, we validate our work with a case-study. By clustering our building-level prediction of Visual Capital directly, we generate view-based boundaries that capture groupings of buildings with similar visual landscapes unbound by administrative boundaries.

Visual landscape quality, and changes to it, have a direct influence on urban planning, policy decisions and individual preferences. Yet, assessing and quantifying visual quality on a large scale remains a challenge. Overcoming this limitation, visual capital provides an easily accessible indicator of a building's visual landscape quality. It thus enables studies that aim to identify correlates with a 'good' view; improve automated real estate valuation models, or quantify the visual impacts of new landscape and urban development projects.

CRediT authorship contribution statement

Adam R. Swietek: Conceptualization, Formal analysis, Investigation, Visualization, Writing – original draft, Writing – review & editing. **Marius Zumwald:** Data curation, Writing – review & editing.

Declaration of Competing Interest

The authors declare the following financial interests/personal relationships which may be considered as potential competing interests: Dr. Marius ZUMWALD is an employee of Wüest Partner.

Data availability

Privacy protected version of the dataset used in the current study is available at https://www.visualcapital.xyz/

Acknowledgements

This project has received funding from the European Union's Horizon 2020 research and innovation programme under the Marie Skłodowska-Curie grant agreement No. 754354. The authors would like to thank Jacqueline Schweizer and the Wüest Partner team for the provision of data and for supporting this research. We thank Prof. Philippe Thalmann and the LEURE team for their helpful discussions.

Appendix A. Supplementary data

Supplementary data to this article can be found online at https://doi.org/10.1016/j.landurbplan.2023.104880.

References

Anselin, L. (1995). Local indicators of spatial association—LISA. *Geographical Analysis, 27*(2), 93–115. https://doi.org/10.1111/j.1538-4632.1995.tb00338.x
Assouline, D., Mohajeri, N., & Scartezzini, J.-L. (2017). Quantifying rooftop photovoltaic solar energy potential: A machine learning approach. *Solar Energy, 141*, 278–296. https://doi.org/10.1016/j.solener.2016.11.045
Baranzini, A., & Schaerer, C. (2011). A sight for sore eyes: Assessing the value of view and land use in the housing market. *Journal of Housing Economics, 20*(3), 191–199. https://doi.org/10.1016/j.jhe.2011.06.001
Biljecki, F., & Chow, Y. S. (2022). Global building morphology indicators. *Computers, Environment and Urban Systems, 95*, Article 101809. https://doi.org/10.1016/j.compenvurbsys.2022.101809
Biljecki, F., & Ito, K. (2021). Street view imagery in urban analytics and GIS: A review. *Landscape and Urban Planning, 215*, Article 104217. https://doi.org/10.1016/j.landurbplan.2021.104217
Biljecki, F., Stoter, J., Ledoux, H., Zlatanova, S., & Çöltekin, A. (2015). Applications of 3D city models: State of the art review. *ISPRS International Journal of Geo-Information, 4*(4), 2842–2889. https://doi.org/10.3390/ijgi4042842
Bosker, M., & Buringh, E. (2017). City seeds: Geography and the origins of the European city system. *Journal of Urban Economics, 98*, 139–157. https://doi.org/10.1016/j.jue.2015.09.003
Breiman, L. (2001). Random forests. *Machine Learning, 45*(1), 5–32. https://doi.org/10.1023/A:1010933404324
Buchak, G., Matvos, G., Piskorski, T., & Seru, A. (2020, December). *Why is intermediating houses so difficult? Evidence from iBuyers* [Working Paper]. National Bureau of Economic Research. doi: 10.3386/w28252.
Buffat, R., Froemelt, A., Heeren, N., Raubal, M., & Hellweg, S. (2017). Big data GIS analysis for novel approaches in building stock modelling. *Applied Energy, 208*, 277–290. https://doi.org/10.1016/j.apenergy.2017.10.041
Burchfield, M., Overman, H. G., Puga, D., & Turner, M. A. (2006). Causes of sprawl: A portrait from space. *The Quarterly Journal of Economics, 121*(2), 587–633. https://doi.org/10.1162/qjec.2006.121.2.587
Chen, M., Liu, Y., Arribas-Bel, D., & Singleton, A. (2022). Assessing the value of user-generated images of urban surroundings for house price estimation. *Landscape and Urban Planning, 226*, Article 104486. https://doi.org/10.1016/j.landurbplan.2022.104486
Chen, T., & Guestrin, C. (2016). XGBoost: A scalable tree boosting system. *Proceedings of the 22nd ACM SIGKDD International Conference on Knowledge Discovery and Data Mining*, 785–794. San Francisco California USA: ACM. doi: 10.1145/2939672.2939785.
Chetty, R., Jackson, M. O., Kuchler, T., Stroebel, J., Hendren, N., Fluegge, R. B., … Wernerfelt, N. (2022). Social capital I: Measurement and associations with economic mobility. *Nature, 608*(7921), 108–121. https://doi.org/10.1038/s41586-022-04996-4
Couture, V., Gaubert, C., Handbury, J., & Hurst, E. (2023). Income growth and the distributional effects of urban spatial sorting. *The Review of Economic Studies*. , Article rdad048. https://doi.org/10.1093/restud/rdad048
Dambon, J. A., Sigrist, F., & Furrer, R. (2021). Maximum likelihood estimation of spatially varying coefficient models for large data with an application to real estate price prediction. *Spatial Statistics, 41*, Article 100470. https://doi.org/10.1016/j.spasta.2020.100470
Federal Office of Topography swisstopo. (2018a). SwissALTI3D. Retrieved December 5, 2022, from Federal Office of Topography swisstopo website: https://www.swisstopo.admin.ch/en/geodata/height/alti3d.html.
Federal Office of Topography swisstopo. (2018b). SwissTLM3D. Retrieved April 6, 2023, from Federal Office of Topography swisstopo website: https://www.swisstopo.admin.ch/en/geodata/landscape/tlm3d.html.
Federal Statistical Office. (2000). Federal Statistical Office. Retrieved November 15, 2022, from https://www.bfs.admin.ch/bfs/en/home.html.
Federal Statistical Office. (2022, February 1). Durchschnittliches steuerbares Einkommen pro Steuerpflichtigem/-r (Kantone/Politische Gemeinden) | Karte. Retrieved September 21, 2022, from Bundesamt für Statistik website: https://www.bfs.admin.ch/asset/de/21324555.
Inglis, N. C., Vukomanovic, J., Costanza, J., & Singh, K. K. (2022). From viewsheds to viewscapes: Trends in landscape visibility and visual quality research. *Landscape and Urban Planning, 224*, Article 104424. https://doi.org/10.1016/j.landurbplan.2022.104424
Kang, N., & Liu, C. (2022). Towards landscape visual quality evaluation: Methodologies, technologies, and recommendations. *Ecological Indicators, 142*, Article 109174. https://doi.org/10.1016/j.ecolind.2022.109174
Ke, G., Meng, Q., Finley, T., Wang, T., Chen, W., Ma, W., … Liu, T.-Y. (2017). LightGBM: A Highly Efficient Gradient Boosting Decision Tree. *Proceedings of the 31st International Conference on Neural Information Processing Systems*, 3149–3157. Red Hook, NY, USA: Curran Associates Inc.
Ko, W. H., Schiavon, S., Altomonte, S., Andersen, M., Batool, A., Browning, W., … Wienold, J. (2022). Window view quality: Why it matters and what we should do. *LEUKOS, 18*(3), 259–267. https://doi.org/10.1080/15502724.2022.2055428
Law, S., Paige, B., & Russell, C. (2019). Take a look around: Using street view and satellite images to estimate house prices. *ACM Transactions on Intelligent Systems and Technology, 10*(5), 1–19. https://doi.org/10.1145/3342240
Lee, S., & Lin, J. (2018). Natural amenities, neighbourhood dynamics, and persistence in the spatial distribution of income. *The Review of Economic Studies, 85*(1), 663–694. https://doi.org/10.1093/restud/rdx018
Lindenthal, T. (2020). Beauty in the eye of the home-owner: Aesthetic zoning and residential property values. *Real Estate Economics, 48*(2), 530–555. https://doi.org/10.1111/1540-6229.12204
Lindenthal, T., & Johnson, E. B. (2021). Machine learning, architectural styles and property values. *The Journal of Real Estate Finance and Economics.*. https://doi.org/10.1007/s11146-021-09845-1
Long, J., & Robertson, C. (2018). Comparing spatial patterns. *Geography Compass, 12*(2), e12356.
Lundberg, S. M., & Lee, S.-I. (2017). A unified approach to interpreting model predictions. *Proceedings of the 31st International Conference on Neural Information Processing Systems*, 4768–4777. Red Hook, NY, USA: Curran Associates Inc.
McInnes, L., Healy, J., & Astels, S. (2017). hdbscan: Hierarchical density based clustering. *Journal of Open Source Software, 2*(11), 205. https://doi.org/10.21105/joss.00205
Milojevic-Dupont, N., Wagner, F., Nachtigall, F., Hu, J., Brüser, G. B., Zumwald, M., … Creutzig, F. (2023). EUBUCCO v0.1: European building stock characteristics in a common and open database for 200+ million individual buildings. *Scientific Data, 10*(1), 147. https://doi.org/10.1038/s41597-023-02040-2
Ögçe, H., Müderrisoğlu, H., & Uzun, S. (2020). Visual impact assessment of the Istanbul Land-wall. *Indoor and Built Environment, 29*(10), 1359–1373. https://doi.org/10.1177/1420326X19874453
Oh, K. (1998). Visual threshold carrying capacity (VTCC) in urban landscape management: A case study of Seoul, Korea. *Landscape and Urban Planning, 39*(4), 283–294. https://doi.org/10.1016/S0169-2046(97)00085-6
Roth, M., Hildebrandt, S., Röhner, S., Tilk, C., Schwarz-von Raumer, H.-G., Roser, F., & Borsdorff, M. (2018). Landscape as an area as perceived by people: Empirically-based nationwide modelling of scenic landscape quality in Germany. *Journal of Digital Landscape Architecture, 3*, 129–137.
Saiz, A. (2010). The geographic determinants of housing supply. *The Quarterly Journal of Economics, 125*(3), 1253–1296. https://doi.org/10.1162/qjec.2010.125.3.1253
Schutte, N. S., & Malouff, J. M. (1986). Preference for complexity in natural landscape scenes. *Perceptual and Motor Skills, 63*(1), 109–110. https://doi.org/10.2466/pms.1986.63.1.109
Sinha, P., Caulkins, M., & Cropper, M. (2021). The value of climate amenities: A comparison of hedonic and discrete choice approaches. *Journal of Urban Economics, 126*, Article 103371. https://doi.org/10.1016/j.jue.2021.103371
Turan, I., Chegut, A., Fink, D., & Reinhart, C. (2020). The value of daylight in office spaces. *Building and Environment, 168*, Article 106503. https://doi.org/10.1016/j.buildenv.2019.106503
Turan, I., Chegut, A., Fink, D., & Reinhart, C. (2021). Development of view potential metrics and the financial impact of views on office rents. *Landscape and Urban Planning, 215*, Article 104193. https://doi.org/10.1016/j.landurbplan.2021.104193
Ulrich, R. S. (1977). Visual landscape preference: A model and application. *Man-Environment Systems, 7*(5), 279–293.
Ulrich, R. S. (1981). Natural versus urban scenes: Some psychophysiological effects. *Environment and Behavior, 13*(5), 523–556. https://doi.org/10.1177/0013916581135001
Ulrich, R. S. (1986). Human responses to vegetation and landscapes. *Landscape and Urban Planning, 13*, 29–44. https://doi.org/10.1016/0169-2046(86)90005-8
Walch, A., Castello, R., Mohajeri, N., & Scartezzini, J.-L. (2020). Big data mining for the estimation of hourly rooftop photovoltaic potential and its uncertainty. *Applied Energy, 262*, Article 114404. https://doi.org/10.1016/j.apenergy.2019.114404
Walz, U., & Stein, C. (2018). Indicator for a monitoring of Germany's landscape attractiveness. *Ecological Indicators, 94*, 64–73. https://doi.org/10.1016/j.ecolind.2017.06.052
Yamagata, Y., Murakami, D., Yoshida, T., Seya, H., & Kuroda, S. (2016). Value of urban views in a bay city: Hedonic analysis with the spatial multilevel additive regression (SMAR) model. *Landscape and Urban Planning, 151*, 89–102. https://doi.org/10.1016/j.landurbplan.2016.02.008
Ye, V. Y., & Becker, C. M. (2018). The Z-axis: Elevation gradient effects in Urban America. *Regional Science and Urban Economics, 70*, 312–329. https://doi.org/10.1016/j.regsciurbeco.2017.10.002
Yu, S., Chen, Z., Yu, B., Wang, L., Wu, B., Wu, J., & Zhao, F. (2020). Exploring the relationship between 2D/3D landscape pattern and land surface temperature based on explainable eXtreme Gradient Boosting tree: A case study of Shanghai, China.

Science of The Total Environment, 725, Article 138229. https://doi.org/10.1016/j.scitotenv.2020.138229

Yu, S., Yu, B., Song, W., Wu, B., Zhou, J., Huang, Y., … Mao, W. (2016). View-based greenery: A three-dimensional assessment of city buildings' green visibility using Floor Green View Index. *Landscape and Urban Planning, 152*, 13–26. https://doi.org/10.1016/j.landurbplan.2016.04.004

Zekar, A., Milojevic-Dupont, N., Zumwald, M., Wagner, F., & Creutzig, F. (2023). Urban form features determine spatio-temporal variation of ambient temperature: A comparative study of three European cities. *Urban Climate, 49*, Article 101467. https://doi.org/10.1016/j.uclim.2023.101467